Materials Science and Engineering A 390 (2005) 13–18

www.elsevier.com/locate/msea

Extended solubility in non-equilibrium Pb/Fe system

E. Nunes [a], E.C. Passamani [a,*], C. Larica [a], J.C.C. Freitas [a], A.Y. Takeuchi [a,b], E. Baggio-Saitovitch [b], A.C. Doriguetto [c], A.A.R. Fernandes [a]

[a] *Universidade Federal do Espírito Santo, Depto. de Física, Vitória, ES 29060-900 Brazil*
[b] *Centro Brasileiro de Pesquisas Físicas, Rio de Janeiro, RJ 22290-180 Brazil*
[c] *Universidade de São Paulo, Instituto de Física, São Carlos, SP 13560-970 Brazil*

Received 24 November 2003; received in revised form 6 May 2004; accepted 12 May 2004

Abstract

Nanostructured Pb/Fe alloys have been produced by means of mechanosynthesis and co-deposition methods in powder and film forms, respectively, in both sides of the composition range. Low temperature Mössbauer results obtained from the films have indicated the presence of interstitial Fe in fcc-Pb lattice, with maximum Fe solubility of 3 at.%. This Fe configuration has an atomic diffusion effect with increasing temperature, resulting in formation of small Fe clusters. On the other hand, milling Fe and Pb powders mixture up to 700 h only produced iron-rich Pb/Fe phases with high degree of chemical disorder established due to different atomic radii of Pb and Fe, as shown by a broad Mössbauer subspectra. The milling procedure extended the Pb solubility limit in Fe matrix to 6 at.%. Therefore, our results of films and milled powders indicated that one has extended the known solubility limit for this system.

Keywords: Metastable phases; Mössbauer effect; Thermal properties; Lead and iron alloys; Milling; Vapor quenching

1. Introduction

Recent development in materials research has paid special emphasis in metastable materials obtained from systems with positive heat of mixing (ΔH). Since the 80s, vapor quenching (VQ), based on sputtering and thermal evaporation techniques, has been used to obtain metastable alloys from immiscible elements. As widely reported, the VQ method increases the solubility range among the alloy components and metastable phases are mostly formed outside the equilibrium range [1,2]. In the 90s, mechanical alloying (MA) process has also been largely employed to produce metastable phases from systems with $\Delta H > 0$ [3–5]. Alloy formation by MA is mainly related to diffusion process at layers interface of the mixed component powders, induced by mechanical energy. Scanning electron microscopy [6] has shown that the repeated fracture and cold welding of powder particles during milling generate a multilayer structure. Subsequently, interdiffusion effect, which takes place at the interface layers, leads to the alloy formation.

Pb and Fe are known to be completely immiscible in the solid state and a small solubility at the composition range edges occurs in the liquid state. In the equilibrium state, the solubility of Fe in liquid Pb at 873 K is about 2.7×10^{-4} at.% [7], while for Pb in liquid Fe is about 5.0×10^{-2} at.% in the range of 1823–1873 K [8]. This is one of the binary immiscible Fe-based systems for which studies have been seldom reported [9,10]. The Pb–Fe system is, therefore, a natural candidate for tentative preparation of alloys using techniques that can yield non-equilibrium phases.

In the present work, vapor quenching and high energy milling (mechanosynthesis) techniques have been combined to study the solubility limit of metastable Pb/Fe alloys in the Fe and Pb sides of the composition range. X-ray diffractometry (XRD), differential scanning calorimetry (DSC) and Mössbauer spectroscopy techniques were used to investigate the features of the alloy formation and its thermal stability.

2. Experimental

Using two non-conventional preparation methods Pb/Fe alloys were produced. For low Fe compositions ($\leq$40 at.%),

* Corresponding author. Fax: +55 27 335 2823.
E-mail address: edson@cce.ufes.br (E.C. Passamani).

0921-5093/$ – see front matter © 2004 Elsevier B.V. All rights reserved.
doi:10.1016/j.msea.2004.05.032

Pb/Fe thin films were prepared using thermal evaporation technique; while for high Fe content (≥90 at.%) mechanosynthesis method was applied. ^{57}Fe atoms in quenched-Pb films were produced in a He-cryostat by thermal co-evaporation of iron (90% enriched in ^{57}Fe) and high purity Pb (99.99%) metals from two independent resistively heated Ta crucibles. The deposition was performed onto kapton substrates kept, during the evaporation, at a temperature close to 20 K. Before the depositions, the vacuum in the cryostat was 9×10^{-9} mbar and about 7×10^{-8} mbar during sample preparation. Crystal oscillators were used to control the deposition rates and the films composition. The films thickness were smaller than or equal to 2000 Å, depending on the total ^{57}Fe concentration. The details of the evaporation set-up have been given elsewhere [11].

Nanostructured Pb_xFe_{1-x} ($x \leq 0.10$) alloys were prepared by mechanosynthesis from the mixture of high purity chemical elemental powders of Fe and Pb (99.999%). The initial powder mixtures were sealed in a hard steel vial under high purity Ar atmosphere (5N5) and clamped in a commercial vibrating frame machine. A massive cylinder made of the same material as the vial was used as milling tool, occupying 63% of total internal volume space. In order to prevent contamination from the milling tools, small amounts of Fe and Pb powders mixture with defined composition were milled in a first run, since these powders will partially cover the milling tool and vial walls. After that, the excess of powder is removed from the vial and new portions of Fe and Pb powders, at desired compositions, are added to the vial, keeping the mass ratio of tool to sample at about 20:1. The milling process extended for periods up to 700 h. More details of the milling tools and experimental procedures have already been reported by Larica et al. [12]. The alloying process has been investigated from the milled powders collected at pre-defined times. Powder manipulation is always done inside a glove box under high purity argon atmosphere to avoid oxidation. Portions of the final milled Pb_xFe_{1-x} alloys were heat-treated in a high vacuum furnace to temperatures up to 700 K, with a residence time of 1 h at the final temperatures.

No XRD analysis was possible to be performed in the case of the films, since they oxidized easily even at the deposition place when the cryostat pressure increased above 10^{-4} mbar. XRD patterns were obtained at room temperature for all samples prepared by MA, using Cu Kα radiation with a Rigaku diffractometer.

Scanning electron microscopy (SEM) and energy dispersive X-ray spectroscopy (EDS) analysis have been used to check the compositions of some final alloys (milled up to 700 h). Within the sensibility of EDS analysis, besides the presence of Fe and Pb, no other elements were detected in the final milled samples and the compositions remained close to the nominal values.

Differential scanning calorimetry analyses were performed in a Shimadzu DSC-50 equipment, between 300 and 723 K. About 10 mg of the milled materials were enclosed in an aluminum pan covered with an aluminum lid (an empty pan with lid was used as reference). The signal was recorded in a heating ramp, with a heating-rate of 20 K/min under an Ar flux of 30 ml/min. The raw DSC data were baseline corrected through the subtraction of the signal obtained with two identical empty pans placed on the reference and sample positions of the calorimeter. The obtained curve was then manually corrected in order to give a flat baseline on both sides of the melting transition of the Pb-rich phases.

The films were analyzed by in situ Mössbauer spectroscopy performed in the transmission geometry, in the temperature range between 7 and 300 K, using a 50 mCi ^{57}Co in Rh matrix radioactive source moving in sinusoidal mode. Source and absorber were kept at the same temperature during the measurements. The Mössbauer spectra of films with low Fe content were fitted using two crystalline subspectra.

The spectra of the milled powders were also recorded in the conventional transmission geometry at 300 K and at 12 K, using a 25 mCi ^{57}Co in Rh matrix radioactive source, moving in triangular mode. The Mössbauer measurements at 12 K have been performed in an APD closed cycle refrigerator. During such measurements the Mössbauer radioactive source was kept at 300 K, while the absorber was at 12 K. The 12 and 300 K spectra have similar aspect and they were fitted with two magnetic subspectra. The final analysis accounted for the expected increase in the magnetic hyperfine field (B_{hf}) values and the second order Doppler effect contribution to the isomer shift (IS). The relative absorption areas of the two magnetic phases observed in the Mössbauer spectra are nearly temperature independent, indicating that these phases have similar Debye Waller factors (f). The IS values of our data are given relatively to α-Fe at 300 K.

3. Results and discussion

As already mentioned in the experimental section, the $Pb_{100-x}Fe_x$ alloys with $x \leq 40$ were prepared using the vapor quenching process on substrate kept at 20 K. For high Fe content ($x \geq 80$), the films could not be produced due to a technical restriction. Also milling method was tentatively used to prepare low Fe content alloys ($x \leq 10$), but the Pb powder particles welded together just after the milling has started, avoiding reaction among the components to take place even for a very long milling times ($Tm > 500$ h).

A set of Mössbauer spectra, recorded in the temperature range from 7 to 190 K and cycling back to 7 K, is displayed in Fig. 1 for a typical film ($Pb_{97}Fe_3$). The spectrum recorded at 300 K is also shown for comparison.

The 7 K Mössbauer spectrum of the 3 at.% Fe film, recorded with a high velocity scale (not shown), has not displayed the presence of any magnetic components, indicating that: (i) Fe atoms are completely dissolved into the Pb matrix, forming a Pb/Fe alloy; (ii) the Fe-containing

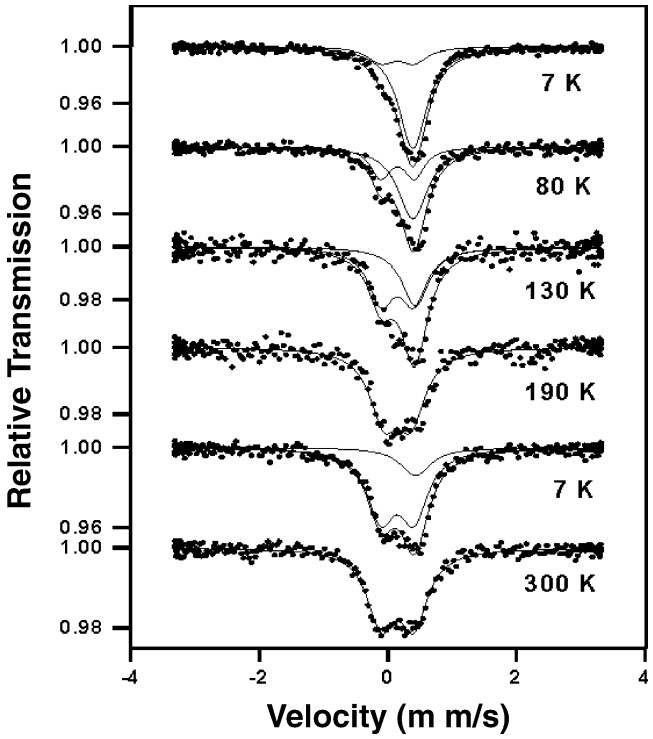

Fig. 1. Temperature dependence of the Mössbauer spectra of the $Pb_{97}Fe_3$ film in one thermal cycle, starting from the top spectrum to the bottom of the figure.

phases present in this sample are not magnetically ordered at 7 K. This film measured under the same conditions, but with low velocity scale (Fig. 1 top spectrum), shows a broad asymmetric paramagnetic spectrum. The spectrum has been analyzed with two paramagnetic subspectra, one singlet and one doublet, having volumetric fractions of 85 and 15%, respectively. The temperature dependence of the spectra displayed in the Fig. 1 shows that the relative absorption area of the doublet increases at the expense of the singlet. At 190 K, only the doublet is observed in the spectrum. A new Mössbauer spectrum recorded at 7 K, after cooling from 190 K, still displays the two subspectra, but their relative intensity values have almost reversed. The presence of the residual singlet at 7 K and its absence at 190 K may indicate that the Debye temperature of the Fe atoms in the cubic configuration is lower than that of Fe atoms related to the doublet. The Debye temperature of Fe in Pb has already been reported to be lower than 150 K for Sielemann [13]. At 300 K, the spectrum shows only the doublet. Based on the diffusion process and the similarity of our results with those reported by Sielemann [13], one might associate the singlet to Fe atoms located at interstitial Pb sites. On the other hand, the observed doublet (D1) is attributed to small Fe clusters (dimmers, trimmers, etc.) originated as consequence of atomic diffusion process or/and due to Fe atoms located at the Pb grain boundaries.

Films with 5 to 20 at.% Fe content have Mössbauer spectra composed by the two components above discussed plus a

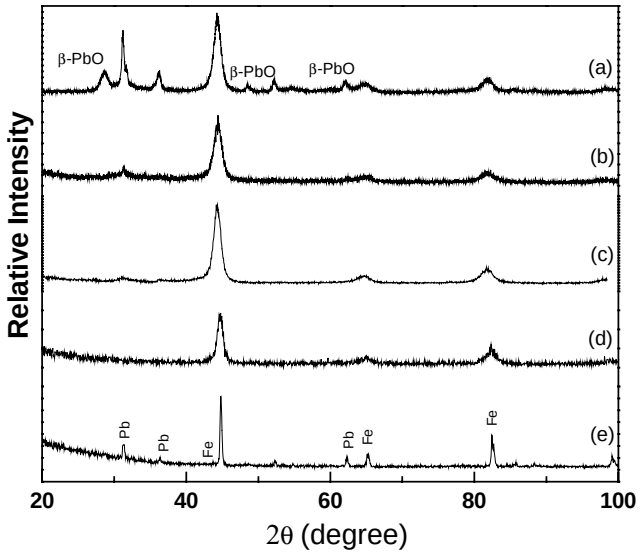

Fig. 2. Room temperature X-ray diffraction patterns of the $Pb_{100-x}Fe_x$ alloys milled for different times (*Tm*): (a) $x = 90$ and $Tm = 700$ h; (b) $x = 93$ and $Tm = 700$ h; (c) $x = 95$ and $Tm = 600$ h; (d) $x = 98$ and $Tm = 224$ h and; (e) non-milled $x = 95$.

magnetic subspectrum with hyperfine parameters close to those of the α-Fe phase. Also, the Mössbauer results of the $x = 40$ film indicate the presence of small magnetic Fe particles [9]. Based on these results one may assure that the Pb and Fe solubility limit, in the Pb-rich side, has been extended in the solid state, compared to that reported for the equilibrium phase diagram.

Fig. 2 shows the XRD patterns of the $Pb_{100-x}Fe_x$ ($x = 98$, 95, 93 and 90) alloys milled for different times (*Tm*). Also, the XRD pattern of a non-milled sample ($x = 95$) was added

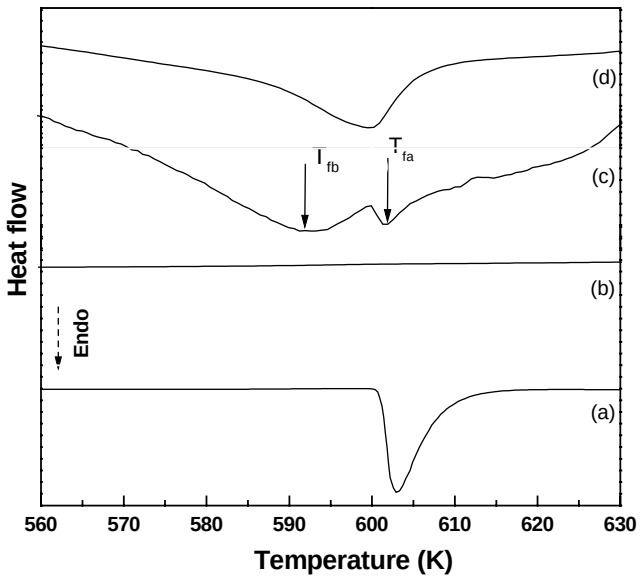

Fig. 3. DSC curves of the $Pb_{100-x}Fe_x$ alloys milled for different times (*Tm*): (a) $x = 90$ and $Tm = 700$ h; (b) $x = 93$ and $Tm = 700$ h; (c) $x = 95$ and $Tm = 600$ h and; (d) non-milled $x = 95$.

for comparison. The XRD pattern of the non-milled sample displays the Bragg reflection lines of the fcc Pb and the bcc-Fe phases. PbO oxide was only detected in the XRD pattern of the sample with 90 at.% of Fe ($x = 90$) and milled for 700 h (Fig. 2a). The main milling effect observed in these XRD patterns is the broadening of the fcc and bcc Bragg peaks and also a shift to lower angles of the α-Fe peaks. The line broadening observed in both structure peaks can be associated with grain refinement as well as to an increase of lattice strain created by the milling process. Grain size values were estimated from the inverse linewidth of the main bcc Bragg peak, using the Scherrer formula. The obtained grain size values were not corrected for lattice defects and instrumental broadening, which means that they may be underestimated. It is worth to say that there is a considerable reduction of the bcc grain sizes with increase of milling time, reaching values as low as 10 nm. On the other hand, the shift effect observed in the Fe peaks may be attributed to a partial substitution of Fe by Pb atoms, into the Fe matrix, leading to an increase in the bcc lattice parameter. From the bcc Bragg peaks, one estimates the lattice parameter to be about 0.292 nm, for the alloy with Pb content of 5 at.%, nearly 2% increase.

Fig. 3 shows DSC curves of the milled $Pb_{100-x}Fe_x$ ($x = 95$, 93 and 90) samples in the temperature range that covers the melting point of the Pb phase. DSC curve of a reference sample (non-milled) is also presented in Fig. 3(d).

For the non-milled sample, the DSC curve displays an endothermic peak starting at 605 K associated with the melting of metallic Pb. For samples with Fe content ≥95 at.% and milled for times above 500 h, no trace of Pb melting has been observed, indicating the absence of free metallic Pb in these samples (see, for an example, the flat DSC line shown in Fig. 3b). On the other hand, one sees the contribution of free Pb phase for samples with concentration lower than 95 at.% of Fe, even at very long milling times, such as 700 h. The DSC curves recorded for these samples Fig. 3c and 3d) exhibit a severely broadened and distorted melting transition, which is associated with the size reduction and structural disorder introduced in the Pb structure by the milling process. The two endothermic peaks at T_{fa} and T_{fb}, as indicated by the arrows in Fig. 3(c), have been previously discussed by Nunes et al. [10] and Sheng et al. [14]. They were associated with bulk-Pb (T_{fa}) and with surface or small Pb-grains (T_{fb}) melting points. Therefore, the absence of free metallic Pb phase in the samples with Pb content ≤5 at.% may be attributed to the formation of a Pb/Fe phase. This attribution will be better discussed in connection with the results of Mössbauer spectroscopy presented below.

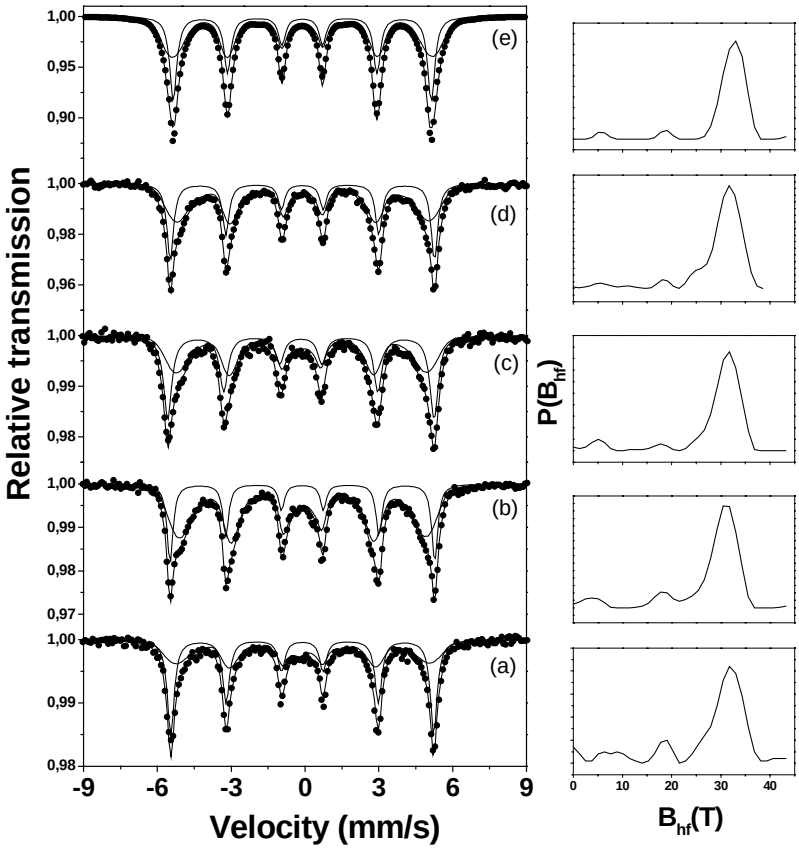

Fig. 4. Room temperature ^{57}Fe Mössbauer spectra of the $Pb_{100-x}Fe_x$ alloys milled for different times (*Tm*): (a) $x = 90$ and $Tm = 700$ h; (b) $x = 93$ and $Tm = 700$ h; (c) $x = 95$ and $Tm = 600$ h; (d) $x = 96$ and $Tm = 700$ h and; (e) $x = 98$ and $Tm = 400$ h. The hf distribution curves are shown on the right.

Mössbauer spectra of the milled $Pb_{100-x}Fe_x$ ($x = 98$, 96, 95, 93 and 90) alloys are presented in Fig. 4. All spectra have six lines due to the magnetic nuclear Zeeman effect. In general, they were analyzed using two magnetic components one of them having the hyperfine parameters close to those of α-Fe (S1), but with increased linewidths (15%) as compared to the corresponding subspectrum of the non-milled sample. The broadening phenomenon observed in the S1 component can be attributed to the increase of lattice defects originated by the milling process and/or to the presence of Pb atoms in the α-Fe matrix. The second magnetic component (S2) is fitted with a magnetic field distribution, which has its most probable magnetic hyperfine field (B_{hf}) value significantly smaller than that of bulk α-Fe. The obtained hyperfine parameter values for the S2 subspectrum are 0.06 (2) mm/s and 31 (1) T of the most probable isomer shift and magnetic field values, respectively. It should be stressed that no Fe oxides have been detected in the milled samples. Another important point that should be remarked here is that the relative fraction of the S2 subspectrum does not scale with Pb composition, indicating that there is a defined solubility limit in the low Pb case, likewise as observed in the high Pb content one.

The presence of α-Fe in the milled samples (S1 subspectrum) requires that the formed Pb/Fe phase has a higher Pb content than the initial non-milled composition. Considering the relative absorption areas of S1 and S2 subspectra and assuming that the broadening of the S1 subspectrum is mostly due to lattice defects and, therefore, that all Pb atoms were consumed to form a Pb/Fe phase, then it may be estimated that the formed phase composition has $x = 94 \pm 1$, for samples with $x \geq 95$ (or Pb content smaller than or equal to 5 at.%).

In a previous work on the milling of Fe and Pb powders with composition $Fe_{95}Pb_5$ using a different milling machine, the formation of a Pb/Fe phase with 29 at.% Pb has been suggested by Nunes et al. [10]. However, the presence of Fe oxides in that sample brings some doubt about the exactness of that result, as the oxidation of Pb is also likely to have occurred in that case. On the other hand, the present samples exhibit no evidence of Fe oxidation (see Mössbauer spectra in Fig. 4) and therefore the estimation given here for the composition of the Pb/Fe phase (around 6 at.% of Pb) seems to be much more reliable.

Thermal stability of milled Pb/Fe alloys has also been investigated using DSC measurement. Fig. 5 shows the DSC curve of non-milled alloy (Fig. 5c) and two curves (Fig. 5a (first run) and 5b (second run)) for the Pb_4Fe_{96} alloy milled for 700 h. For the non-milled sample, the endothermic peak related to bulk Pb melting is observed. For the milled alloy, the DSC curve shows an irreversible exothermic sharp peak at about 666 K (Fig. 5a) and no endothermic peak associated with free metallic Pb, as already discussed above. No significant endo- or exothermic effect are noted in the second DSC scan (Fig. 5b). Mössbauer spectrum obtained from the sample after DSC measurements (not shown) only displays

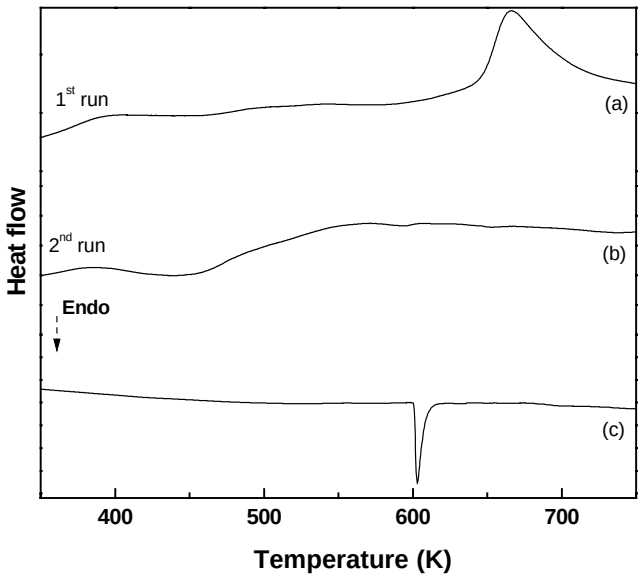

Fig. 5. DSC curves of the Pb_4Fe_{96} sample milled for 700 h and heated up to 700 K twice: (a) first run; (b) second run and; (c) the same sample without milling.

the sextet with α-Fe hyperfine parameter values, indicating that the Pb/Fe phase components have been dissociated at the DSC temperature range, in agreement with the result displayed in Fig. 5(b). The absence of Pb endothermic peak in the second DSC run may be due to the formation of Pb small particles or oxides. The latter has not been observed in the XRD pattern.

In order to better understand the atomic diffusion process observed in Pb/Fe milled alloy, thermal treatments in a Mössbauer vacuum furnace were performed. The Mössbauer spectra of the Pb_7Fe_{93} alloy, as milled ($Tm = 700$ h) and heat-treated at different temperatures, are displayed in Fig. 6. The spectrum of the as-milled sample, as briefly discussed above, was analyzed with two magnetic subspectra plus a small paramagnetic subspectrum associated with Pb/Fe particles in a paramagnetic state. This doublet, present only in this sample, has hyperfine parameters similar to those observed in the film case (D1), where it has been associated with Fe clusters at Pb grain boundaries.

With increasing annealing temperature one may note significant changes in the shape of the S2 subspectrum concomitantly with reduction of its relative fraction. For the first annealing temperature ($T_{ann} = 523$ K), the Mössbauer spectrum shows the presence of a new paramagnetic component (D2) with hyperfine parameters characteristic of Fe oxide. Nevertheless, the fraction of Fe oxide subspectrum (D2) does not increase with increasing temperature, indicating that the oxidation process has taken place only in the first stage of the heat treatment. The presence of Fe oxide may be understood as due to the oxidation of the existing fraction of very small Fe particles, which are sensitive to the residual pressure in the vacuum furnace (as an oxygen getter). The absence of the doublet D2 in the spectrum for the sample

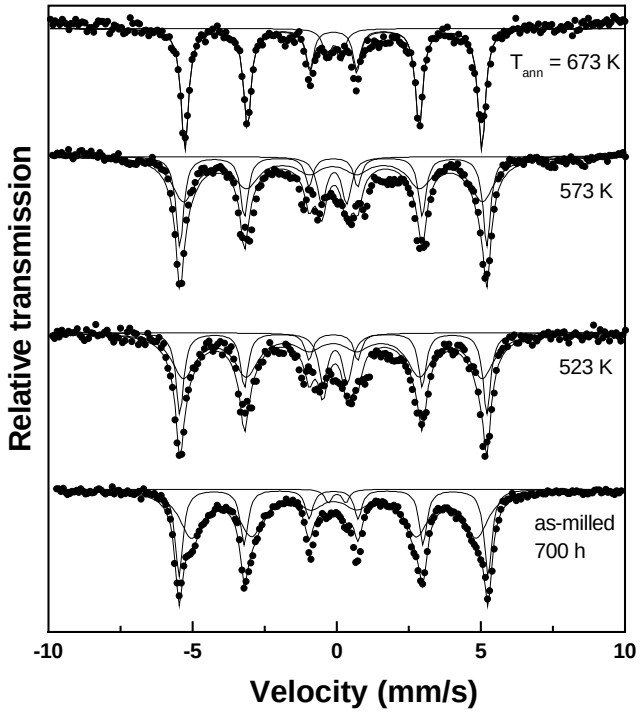

Fig. 6. Room temperature ^{57}Fe Mössbauer spectra of the annealed Pb_7Fe_{93} alloy milled for $Tm = 700$ h. The annealing temperatures (T_{ann}) are indicated in the figure.

annealed at 673 K may be understood, if it is assumed that an increase of the crystal size of Fe oxide particles leads to magnetic ordered state, with the absorption lines dispersed in the background. It should also be stressed that the S2 subspectrum is no longer observed, which is a strong evidence of the metastable Pb/Fe phase thermal instability. The small doublet observed in this spectrum has again the D1 hyperfine parameters, indicating that this phase may be due to small Fe clusters at the Pb grain boundaries. The XRD pattern of the Pb_7Fe_{93} alloy annealed at 673 K (not shown) shows Bragg peaks corresponding to: (i) Fe oxide phase; (ii) fcc Pb Bragg peaks and finally; (iii) very narrow peaks of bcc-Fe phase. Therefore, with the results of the milled and annealed samples one may conclude that Pb atoms dissolve in the bcc-Fe structure up to a limit of 6 at.% Pb.

4. Conclusion

In this work vapor quenching and mechanosynthesis techniques have been applied to produce Pb/Fe alloys with composition in the Fe-rich and Pb-rich sides of the phase diagram. Films with high Fe content ($x \geq 80$) could not be produced due to a technical restriction in our experimental set-up. Also milling process did not produce alloys with low Fe content ($x \leq 10$) because Pb powder particles get welded just after the milling has started avoiding reaction among the components. XRD, DSC and Mössbauer spectroscopy were used to study the formation of the Pb/Fe phase and its transformation during the annealing process. The main results indicate that low Fe concentration Fe/Pb films show formation of a solid solution of 3 at.% of Fe in Pb matrix when the substrate is kept at low temperatures. This configuration under thermal treatments, up to 300 K, leads to the formation of small Fe clusters located at the Pb grain boundaries. The similar doublet (D1) observed for the high Fe contents annealed samples produced by mechanosynthesis gives an additional support to the latter conclusion. For the samples with high Fe composition prepared by milling, the present results indicate the formation of a solid solution with Pb content as high as 6 at.% dissolved in the α-Fe matrix.

Acknowledgements

We acknowledge the financial support of UFES and CNPq for this work as well as FAPERJ (Cientista do Nosso Estado), and MCT/PCI Program at CBPF.

References

[1] C.L. Chien, S.H. Liou, D. Kofalt, Y.u. Wu, T. Egami, T.R. McGuirre, Phys. Rev. B 33 (1986) 3247.
[2] C. Larica, E. Baggio-Saitovitch, S.K. Xia, J. Magn. Magn. Mater. 110 (1992) 106.
[3] A.R. Yavari, P.J. Dere, T. Benameur, Phys. Rev. Lett. 68 (1992) 2235.
[4] N.S. Cohen, Q.A. Pankhurst, L.F. Barquìn, J. Phys. Cond. Mater. 11 (1999) 8839.
[5] S.W. Mahon, X. Song, M.A. Howson, B.J. Hickey, R.F. Cochrane, Mater. Sci. Forum 225–227 (1996) 157.
[6] E. Hellstern, L. Schultz, Appl. Phys. Lett. 48 (1986) 124.
[7] T. Araki, Trans. Natl. Res. Inst. Metals Tokyo 5 (1963) 91.
[8] J. R. Weeks, NASA Special Publication (NASA-SP), Natl. Aeron. Space Admin. 41 (1963) 21.
[9] E.C. Passamani, E. Baggio-Saitovitch, S.K. Xia, C. Larica, J. Phys. C: Cond. Mater. 7 (1995) 8437.
[10] E. Nunes, E.C. Passamani, C. Larica, J.C.C. Freitas, A.Y. Takeuchi, J. Alloys Compd. 345 (2002) 116.
[11] E. Baggio-Saitovitch, V. Drago, H. Micklitz, Proceedings of LACAME'88 (World Scientific, Singapore) (1990) 290.
[12] C. Larica, K.M.B. Alves, E. Baggio-Saitovitch, A.P. Guimarães, J. Magn. Magn. Mater. 145 (1995) 306.
[13] R. Sielemann, Hyp. Int. 80 (1993) 1239.
[14] S.W. Sheng, K. Lu, E. Ma, Acta Mater. 46 (1998) 5195.